

PDE AND TENSOR BASED APPROACH FOR PARIETAL DYNAMIC TRACKING IN ULTRASOUND SEQUENCES

C. Tilmant, L. Sarry, J.-Y. Boire
ERIM, Faculty of Medicine, Clermont-Ferrand, France

Abstract- A method for pericardial and endocardial edge extraction of the left ventricle (LV) in 2-D short axis echocardiographic sequence is presented. The proposed algorithm consists in two steps: nonlinear anisotropic diffusion filtering and directional geodesic active contours. These steps are based on both PDE and tensors. Tensor formalism gives access to structure orientation of the acoustic density field. This provides a more robust algorithm by using the whole image information. Sample experimental results are shown for myocardium edge detection in 2-D short-axis ultrasound sequences.

Keywords - echocardiography, nonlinear anisotropic diffusion, directional geodesic active contours, PDE, tensor.

I. INTRODUCTION

Color kinesis is an echocardiographic technique based on acoustic densitometry to assess parietal movements. It has been designed to make the detection of contraction abnormality easier and is provided as an online tool on ultrasound imaging system (e.g. Hewlett-Packard Sonos 5500). For each frame, every pixel within a ROI outside the LV cavity is classified either as blood or endocardium with respect to its integrated backscatter level. Diastolic endocardial motion is visualized. Class transitions are encoded using a specific color hue for each consecutive frame, each color corresponding to the wall excursion over a 33-ms period of time. Concentric color bands are superimposed on the end-diastolic frame to depict the entire LV endocardial excursion throughout diastole. This technique requires a high image quality in order to detect closed edges. To overcome this limitation, deformable models based on PDE and tensors are used for the tracking of myocardium walls from an ultrasound sequence.

The present paper describes how tensor formalism can be coupled to PDE in a segmentation problem in order to better take into account gray level information than with a gradient.

In section II, we explain the relevance of tensor use, its mathematical framework and the adaptation of algorithms to ultrasound context. Finally section III focuses on results and discussion.

II. METHODOLOGY

Our method can be divided into two parts. First, there is a preprocessing step based on nonlinear anisotropic diffusion. It aims at reducing speckle in the original image without altering its significant features. Secondly, in order to extract myocardium boundaries, a method of directional active contours is used. These processings are based on both tensor and PDE.

A. The Structure Tensor

In case of low contrast or textured images, the use of simple edge detector like the Gaussian smoothed gradient may not be efficient enough. A more sophisticated descriptor is thus required by means of *structure tensor*:

$$\nabla I_{\sigma} \triangleq \nabla (K_{\sigma} * I), \quad (1)$$

where I is the image gray level, K_{σ} a Gaussian kernel with standard deviation σ and $*$ the convolution product. In this case, σ is usually called *local space*.

The previous regularized gradient gives a local direction, but a more relevant information is the orientation. A tensor product is defined by:

$$\mathbf{J}_0(\nabla I_{\sigma}) \triangleq \nabla I_{\sigma}^t (\nabla I_{\sigma}) \quad (2)$$

This matrix owns interesting intrinsic properties. Indeed, its eigenvectors (v_1, v_2) define an orthonormal basis, and the corresponding eigenvalues (μ_1, μ_2) give a measure of contrast at the local scale σ :

$$\begin{aligned} v_1 // \nabla I_{\sigma} & \quad v_2 \perp \nabla I_{\sigma} \\ \mu_1 = |\nabla I_{\sigma}|^2 & \quad \mu_2 = 0 \end{aligned} \quad (3)$$

Finally, the convolution of $\mathbf{J}_0(\nabla I_{\sigma})$ with a Gaussian kernel K_{ρ} gives a local descriptor of gray level orientation called *structure tensor*:

$$\mathbf{J}_{\rho}(\nabla I_{\sigma}) \triangleq K_{\rho} * \mathbf{J}_0(\nabla I_{\sigma}) \quad (4)$$

The standard deviation ρ of this kernel is called the *integration scale*. $\mathbf{J}_{\rho}(\nabla I_{\sigma})$ reflects the image coherence. A geometric interpretation can be inferred from spectral decomposition [11]. Indeed, the eigenvector associated to the highest eigenvalue λ_1 corresponds to the average direction of the maximal gray level variation. Furthermore, the other eigenvector gives the dominant local direction, called *coherence direction*. The eigenvalues ($\lambda_1 \geq \lambda_2 \geq 0$) describe the local configurations of gray levels:

- constant areas: $\lambda_1 \approx \lambda_2 \approx 0$,
- edges: $\lambda_1 \gg \lambda_2 \approx 0$,
- corners: $\lambda_1 \gg \lambda_2 \gg 0$.

Therefore, $\lambda_1 - \lambda_2$ acts as a local measure of anisotropy.

Report Documentation Page

Report Date 25 Oct 2001	Report Type N/A	Dates Covered (from... to) -
Title and Subtitle PDE and Tensor Based Approach for Parietal Dynamic Tracking in Ultrasound Sequences		Contract Number
		Grant Number
		Program Element Number
Author(s)		Project Number
		Task Number
		Work Unit Number
Performing Organization Name(s) and Address(es) ERIM, Faculty of Medicine Clermont-Ferrand, France		Performing Organization Report Number
Sponsoring/Monitoring Agency Name(s) and Address(es) US Army Research, Development & Standardization Group (UK) PSC 802 Box 15 FPO AE 09499-1500		Sponsor/Monitor's Acronym(s)
		Sponsor/Monitor's Report Number(s)
Distribution/Availability Statement Approved for public release, distribution unlimited		
Supplementary Notes Papers from 23rd Annual International Conference of the IEEE Engineering in Medicine and Biology Society, October 25-28, 2001, held in Istanbul, Turkey. See also ADM001351 for entire conference on cd-rom.		
Abstract		
Subject Terms		
Report Classification unclassified	Classification of this page unclassified	
Classification of Abstract unclassified	Limitation of Abstract UU	
Number of Pages 4		

B. Non-Linear Anisotropic Diffusion

Diffusion in image processing is equivalent to a physical process, which aims at equilibrating differences in concentration (Fick's law) under the mass condition conservation. A mathematical formulation leads to the diffusion equation:

$$\partial_t C = \text{div}(\mathbf{D} \nabla C) \quad (5)$$

where C is a concentration and \mathbf{D} a diffusion tensor. This equation is the familiar heat equation in the context of heat transfer.

In image processing, we identify the concentration with the image gray level at a given location. This equation is the starting point of filtering diffusion methods [15]. From all the existing methods, three different classes can be extracted:

- linear isotropic diffusion filter with constant scalar diffusivity [7, 17];
- nonlinear isotropic diffusion filter with scalar diffusivity adapted to the local image structure [4, 10];
- nonlinear anisotropic diffusion filter with diffusion tensor adapted to the local image structure [5, 16].

The nonlinear isotropic diffusion is not suited to ultrasound image because of noisy edges. On the other hand the nonlinear anisotropic diffusion is able to eliminate noise while enhancing edges.

Finally, the model of nonlinear anisotropic diffusion with temporal regularization proposed by Cottet and El-Ayyadi [5] is given by a coupled PDE-ODE system:

$$\begin{aligned} \frac{\partial I}{\partial t} &= \text{div}(\mathbf{D} \nabla I), \\ \frac{d\mathbf{D}}{dt} &= \frac{1}{\tau} (\mathbf{F}_s(\nabla I) - \mathbf{D}). \end{aligned} \quad (6)$$

τ is a diffusion parameter and $\mathbf{F}_s(\nabla I)$ a nonlinear operator of orthogonal projection defined as:

$$\mathbf{F}_s(\nabla I) = \begin{cases} \mathbf{P}_{\text{VL.L}} & \text{if } |\nabla I| \geq s \\ \frac{3}{2} \left(1 - \frac{|\nabla I|^2}{s^2} \right) \mathbf{Id} + \frac{|\nabla I|^2}{s^2} \mathbf{P}_{\text{VL.L}} & \text{if not} \end{cases} \quad (7)$$

with $\mathbf{P}_{\text{VL.L}} = \frac{1}{|\nabla I|^2} \begin{bmatrix} I_y^2 & I_x I_y \\ I_x I_y & I_x^2 \end{bmatrix}$, $\nabla I = \begin{pmatrix} I_x & I_y \end{pmatrix}$,

where s is a contrast parameter which is a threshold on image gradient selecting significant edges.

Operator $\mathbf{P}_{\text{VL.L}}$ can be interpreted as the $+\pi/2$ rotation of $\mathbf{J}_0(\nabla I_\sigma)$. It means that image is diffused along edges perpendicularly to the orientation defined by the structure tensor.

C. Directional Geodesics Actives Contours

The model of geodesic active contour was introduced by Caselles [3] as a geometric alternative for snakes, which are the parametric active contour of Kass *et al* [8].

Snakes are based on an energy minimization along a parametric curve. This energy is composed of an internal term and an external one. Two major problems may be encountered. First, the energy non-convexity does not guarantee the uniqueness of the solution. Secondly, topology changes and singularities are forbidden by the explicit representation.

The geodesic active contours [3] are not only based on an energy minimization, but are also parameter-free thanks to an intrinsic geometric model. Evolution equation uses the level set representation of Osher and Sethian [9]:

$$\begin{aligned} \frac{\partial u}{\partial t} &= |\nabla u| \nabla \cdot \left(g(|\nabla I_\sigma|) \frac{\nabla u}{|\nabla u|} \right) + v g(|\nabla I_\sigma|) |\nabla u| \\ \frac{\partial u}{\partial t} &= g(|\nabla I_\sigma|) |\nabla u| \left(\nabla \cdot \left(\frac{\nabla u}{|\nabla u|} \right) + v \right) + \nabla g(|\nabla I_\sigma|) |\nabla u|. \end{aligned} \quad (8)$$

In this relation u is the implicit contour representation. In the level set formulation, inward unit normal vector of the contour is intrinsically given by $\nabla u / |\nabla u|$ and curvature by $\nabla \cdot (\nabla u / |\nabla u|)$. Concerning boundary detection, the stopping function g is a positive decreasing function of the image gradient. The right hand side of (8) can be interpreted as the contribution of two forces. The first one is linked to the contour geometry, weighted by the stopping function and combines a local contribution (curvature) and a global speed one (inner pressure parameter v). The second one is an attraction term oriented towards edges.

Like snakes, geodesic active contours use only minimal geometric information by means of a first order isotropic estimator $|\nabla I_\sigma|$ associated to the stopping function g : it weights the contour normal speed and is part of the attraction term.

A model of directional geodesic active contour based on tensor formalism is proposed in [11] in order to manage the orientation of local structures. This model can be interpreted as an anisotropic generalization of the geodesic actives contours. The first model of geodesic active contour [3] is generalized by:

$$\frac{\partial u}{\partial t} = |\nabla u| \nabla \cdot \left(\mathbf{D} \frac{\nabla u}{|\nabla u|} \right) + v \sqrt{\det(\mathbf{D})} |\nabla u|, \quad (9)$$

with the following boundary condition:

$$\mathbf{D} \nabla u \cdot \vec{n} = 0 \text{ on } \partial\Omega \times (0, T] \quad (10)$$

where Ω is the image domain. In this PDE, \mathbf{D} is an interaction tensor computed as a function of the image structure tensor.

In order to reflect the image local geometric structure, the eigenvectors of \mathbf{D} have to coincide with those of $\mathbf{J}_g(\nabla I_\sigma)$. Associated eigenvalues are replaced by $g(\lambda_1 - \lambda_2)$ and 1 respectively to specialize contour behavior along the image structure. The interaction tensor \mathbf{D} is a generalization of the edge detector g .

D. Application to parietal tracking in ultrasound sequences

For myocardium segmentation on short-axis view, different approaches are to be used for pericardium and endocardium. Indeed, there are physiologically important differences between these two objects. First, endocardial wall is an interface between blood and muscle with rather high contrast, while pericardium presents a contrast inversion from anterior walls to posterior ones. Secondly, while endocardium has a complex geometry and goes through large topological changes, pericardium shape is less variable throughout the cardiac cycle.

- Pericardium:

After a manual initialization on the first frame, active contour model is used with a zero pressure parameter. Indeed, a small movement assumption is taken into account, for this boundary, *i.e.* contour should stay in the attraction valley of the stopping function between two consecutive frames.

- Endocardium:

For each frame, a seed is put in the middle of the image and pressure parameter v is used in order to push the contour towards the endocardium. But a constant parameter is not relevant, because residual pressure forces could push the contour through low edges. A new parameter depending on the global contour energy is thus introduced:

$$v(u^{-1}(0)(s)) = \text{sign}(\Delta I) \cdot \frac{\oint_{u^{-1}(0)} \sqrt{\det(\mathbf{D}(u^{-1}(0)(s)))} ds}{\oint_{u^{-1}(0)} ds}, \quad (11)$$

where s is the curvilinear abscissa on the curve $u^{-1}(0)$, Δ is the laplacian operator and sign , the sign operator.

The global energy criterion insures that the contour slows down even on weakly constrained segments. Furthermore, the sign of the image laplacian is applied to define a return force oriented towards edges.

The relative stability of $|v|$ is used as a stopping criterion.

In practice, the numerical scheme proposed in [5] is used for the diffusion process. For active contours, the implicit formulation of level-set [9] is used combined to a narrow-band optimization [1].

III. RESULTS AND DISCUSSION

The previous algorithms are applied to IBS (Integrated BackScatter) ultrasound sequences on short-axis view from a Hewlett-Packard Sonos 5500 imaging system. This

acquisition mode is usually used for quantification purposes of cyclic variations (CVs) and provides smoother images. Images are encoded as 512*480 matrices on a 8-bit depth and sequences sampled at a 25 Hz rate.

A. Nonlinear anisotropy diffusion

Figure 1 gives the result of the nonlinear anisotropic diffusion filtering. Three parameters are to be adjusted.

Contrast parameter is chosen to preserve significant edges: a value of 0.25 provides a good enhancement of the endocardial wall. The pericardial wall exhibits a lower contrast not far from the noise level and is thus less pronounced.

The diffusion parameter τ is directly related to the iteration number n . Indeed, it has been proved that the algorithm tends towards a steady state within a few τ . A good compromise between diffusion quality and computational cost is obtained for $\tau = 40$ and $n = 3\tau$.

B. Directional geodesic actives contours

Figure 2 gives an example of endocardium detection. The same process is performed for each frame and the result of the endocardium tracking is shown for the systolic period. Three contours out of seven have been sampled for better visualization.

Concerning pericardium tracking, four consecutive pericardium walls have been drawn on the same image in order to assess its movement during the diastolic period.

Small values of the scale parameters ($\sigma=0.5$, $\rho=0.5$) are chosen for these two tracking steps because of the diffusion preprocessing. In case of higher values, corresponding Gaussian filtering would alter edge information. The new pressure parameter v (11) increases convergence rate.

Whereas endocardial wall tracking is fully automatic, pericardial wall one requires user interaction when the contour is too far from the attraction valley (1 image out of 5 on average).

V. CONCLUSION

A parietal dynamic tracking for ultrasound sequences was presented, which combines a preprocessing step based on a nonlinear anisotropic diffusion filtering and directional geodesic active contours. A 2-D version of the algorithms was presented and a 3-D (2-D+T) generalization is planned for nonlinear anisotropic filtering. At present, this method suffers from high calculation cost and algorithms for both nonlinear anisotropic diffusion filtering and directional geodesic active contour could be improved by using a fast algorithm based on parallel implementations of AOS (Additive Operator Splitting). [6,14]

ACKNOWLEDGMENT

The authors wish to thank Pr. Cassagnes, Pr. Lusson, Dr. Motreff and Dr. Langlade from the department of cardiology of the Gabriel Montpied hospital (Clermont-Ferrand, France) for their support and valuable suggestions.

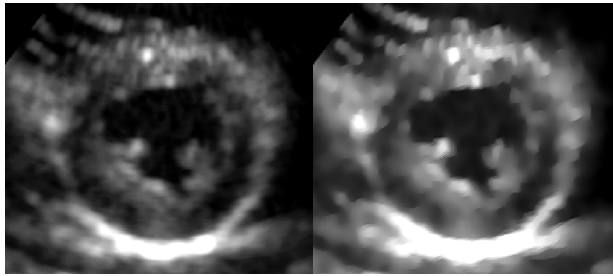


Figure 1 Pre-treatment filtering

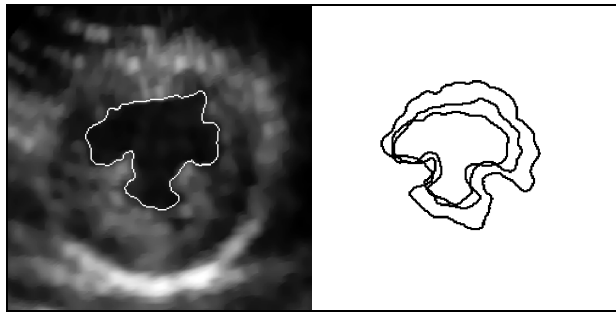


Figure 2 Detection and tracking of endocardium

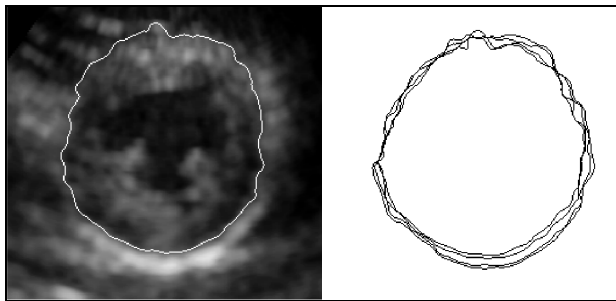


Figure 3 Detection and tracking of pericardium

REFERENCES

- [1] D. Adalsteinsson and J. A. Sethian, "A fast level set method for propagating interfaces," *J. Comput. Phys.*, vol. 118(2), pp. 269-277, 1995.
- [2] V. Caselles, F. Catte, T. Coll, and F. Dibos, "A geometric model for active contours," *Numer. Math.*, vol. 66, pp. 1-31, 1993.
- [3] V. Caselles, R. Kimmel, and G. Sapiro. "On geodesic active contours," *Inter. J. Comput. Vision*, vol. 22(1), pp. 61-79, February 1997.
- [4] F. Catté, P.-L. Lions, J.-M. Morel, T. Coll, "Image selective smoothing and edge detection by nonlinear diffusion," *SIAM J. Numer. Anal.*, vol. 29, pp. 182-193, 1992.
- [5] G.-H. Cottet and M. El Ayyadi, "A Volterra type model for image processing," *IEEE Trans. Image Process.*, vol. 7, 1998.
- [6] R. Goldenberg, R. Kimmel, E. Rivlin and M. Rudzsky. "Fast geodesic active contours" Accepted to *IEEE Trans. Image Process.*, 2001.
- [7] T. Iijima, "Basic theory of pattern normalization (for the case of a typical one-dimensional pattern)," *Bull. Electrotech. Lab.*, vol. 26, pp. 368-388, 1962.
- [8] M. Kass, A. Witkin and D. Terzopoulos, "Snakes : Active contour models," *Inter. J. Comput. Vision*, vol. 1, pp. 321-332, January 1988.
- [9] S. Osher and J. A. Sethian, "Fronts propagating with curvature-dependent speed : Algorithms based on Hamilton-Jacobi formulations," *J. Comput. Phys.*, vol. 118(2), pp. 269-277, 1995.
- [10] P. Perona, J. Malik, "Scale space and edge detection using anisotropic diffusion," *IEEE Trans. Pattern Anal.*, vol. 12, pp. 629-639, 1990.
- [11] N. Rougon and F. Preteux, "Contours actifs généralisés," *Research Report 97.08.01 Institut National des Télécommunications - Département SIM, Evry, France*, August 1997.
- [12] N. Rougon and F. Preteux, "Directional adaptive deformable models for segmentation," *J. Electron. Imaging*, vol. 7(1), pp. 231-256, January 1998.
- [13] J.A. Sethian, "Level set methods and fast marching methods," *Cambridge University Press*, 1999.
- [14] J. Weickert, B. M. ter Haar Romeny and M. A. Viergever "Efficient and reliable scheme for nonlinear diffusion filtering," *IEEE Trans. Image Process.*, vol. 7, pp. 398-410, 1998.
- [15] J. Weickert, "A review of nonlinear diffusion filtering," *B. ter Haar Romeny, L. Florack, J. Koenderink, M. Viergever (Eds.), Scale-Space Theory in Computer Vision, Lecture Notes in Comp. Science*, vol. 1252, Springer, Berlin, pp. 3-28, 1997. Invited paper.
- [16] J. Weickert, "Anisotropic diffusion in image processing," *PhD thesis*, University of Kaiserslautern, 1996.
- [17] A.P. Witkin, "Scale space filtering," *Proc. Eighth Int. Joint Conf. On Artificial Intelligence*, vol. 2, pp. 1019-1022, 1983. [*IJCAI'83, Karlsruhe, August 8-12, 1983*]